Mechanocardiography detects improvement of systolic function caused by resynchronization pacing

Fadime Tokmak[1], Tero Koivisto[1], Olli Lahdenoja[1], Tuija Vasankari[2], Samuli Jaakkola[2], K. E. Juhani Airaksinen[2]

[1] Department of Computing, University of Turku, Vesilinnantie 5, 20500 Turku, Finland
[2] Heart Center, Turku University Hospital, Hämeentie 11, 20520 Turku, Finland

E-mail: fadime.f.tokmak@utu.fi

Abstract

Objective. Cardiac resynchronization therapy (CRT) is commonly used to manage heart failure with dyssynchronous ventricular contraction. CRT pacing resynchronizes the ventricular contraction, while AAI (single-chamber atrial) pacing does not affect the dyssynchronous function. This study compared waveform characteristics during CRT and AAI pacing at similar pacing rates using seismocardiogram (SCG) and gyrocardiogram (GCG), collectively known as mechanocardiogram (MCG). *Approach.* We included 10 patients with HFrEF (Heart Failure with reduced Ejection Fraction) and previously implanted CRT pacemakers. ECG and MCG recordings were taken during AAI and CRT pacing at a heart rate of 80 bpm. Waveform characteristics, including energy, vertical range (amplitude) during systole and early diastole, electromechanical systole (QS2) and left ventricular ejection time (LVET), were derived by considering 6 MCG axes and 3 MCG vectors across frequency ranges of >1 Hz, 20-90 Hz, 6-90 Hz and 1-20 Hz. *Main results.* Significant differences were observed between CRT and AAI pacing. CRT pacing consistently exhibited higher energy and vertical range during systole compared to AAI pacing ($p < 0.05$). However, QS2, LVET and waveform characteristics around aortic valve closure did not differ between the pacing modes. Optimal differences were observed in SCG-Y, GCG-X, and GCG-Y axes within the frequency range of 6-90 Hz. *Significance.* The results demonstrate significant differences in MCG waveforms, reflecting improved mechanical cardiac function during CRT. This information has potential implications for predicting the clinical response to CRT. Further research is needed to explore the differences in signal characteristics between responders and non-responders to CRT.

Keywords: accelerometer, gyroscope, heart failure, resynchronization therapy, smartphone

1. Introduction

Heart failure is a clinical syndrome characterized by dyspnea and exercise intolerance due to impairment of ventricular filling or ejection of blood to circulation or both. Heart failure with reduced ejection fraction (HFrEF) occurs when the left ventricular EF is 40% or less and is accompanied by compensatory ventricular dilatation. Treatment of HFrEF includes the use of evidence based disease-modifying drugs and in selected cases accompanied by device therapies [1]. Dyssynchronic ventricular contraction caused usually by left bundle branch block exacerbates the symptoms and worsens the prognosis in quarter of heart failure patients [2]. Modern cardiac resynchronization therapy (CRT) can, however, synchronize and improve ventricular contraction

leading to improved exercise tolerance, health-related quality of life, and reduced mortality [3]. Unfortunately, up to one third of patients do not get clear benefit of CRT pacing and upfront identification of these patients is difficult [4]. Some of this handicap can be relieved by optimization of pacing settings using electro- and echocardiographic indexes, but at present there is no consensus on which method to use for optimization [4–6].

Mechanocardiography (MCG) including seismocardiography (SCG) and gyrocardiography (GCG) records the microvibrations caused by movements of cardiac mass and blood in the large vessels with micro-accelerometers and gyroscopes placed on body surface [7–9]. In earlier studies, it is shown that a smartphone application using MCG can be used for screening of atrial fibrillation yielding a good diagnostic accuracy compared with devices using photoplethysmography [10]. Previous research has demonstrated that waveforms derived from SCG and GCG reproduce the main events seen in left ventricular twist and strain rate obtained from echocardiography [8,11]. Importantly, abnormalities caused by myocardial infarction and heart failure can also be detected using this technology [12–14]. Clinical data on these techniques in heart failure is still limited, but MCG may help to assess the clinical status of patients with heart failure [15,16]. In this study, we investigated whether MCG could be used to detect improvement of cardiac mechanical function caused by CRT pacing which could be helpful in prediction of the clinical response to CRT.

2. Methods

2.1 Patients

This study is part of MECHANO-HF study - a joint effort of the Heart Center, Turku University Hospital, Turku; and the Department of Computing, University of Turku, Turku, Finland – and included 10 patients with HFrEF and previously implanted CRT pacemaker. The inclusion criteria for the study were: (1) the patient's age at least 18 years, (2) he/she was capable of understanding and willing to sign an informed consent form, (3) and no significant valve disease or rhythm irregularities and stable clinical condition. Baseline characteristics of study population are presented in Table 1. MECHANO-HF studies and the protocol were approved by the Ethics Committee of the Hospital District of Southwest Finland. The study was performed in accordance with the Declaration of Helsinki as revised in 2002. All patients gave their written informed consent.

Variable		
Age (year)	Mean (±SD)	73.98 (±7.52)
Sex	Males, n	8
	Females, n	2
Height (cm)	Mean (±SD)	172.20 (±6.97)
Weight (kg)	Mean (±SD)	92.80 (±22.95)
BMI (kg/m²)	Mean (±SD)	31.00 (±5.59)
Left ventricular ejection fraction (%)*	Mean (±SD)	39.90 (±8.77)
NYHA class	I, n	1
	II, n	4
	III, n	4
	IV, n	1

**After introduction of optimal medical treatment and CRT*

Table 1. Baseline characteristics of patients included in the study. Note that age information was not obtained for one patient and left ventricular ejection fraction was measured after treatment.

2.2 Data Acquisition

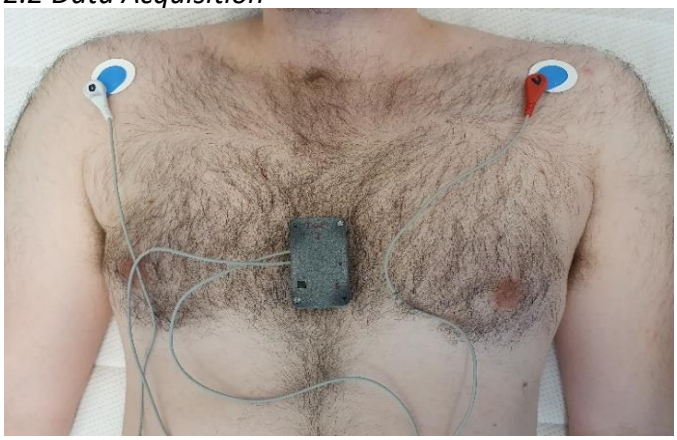

Figure 1 The device is placed on the patient's lower portion of the chest, measuring 3-axis acceleration, 3-axis rotation, and one lead ECG while the patient lies in supine position.

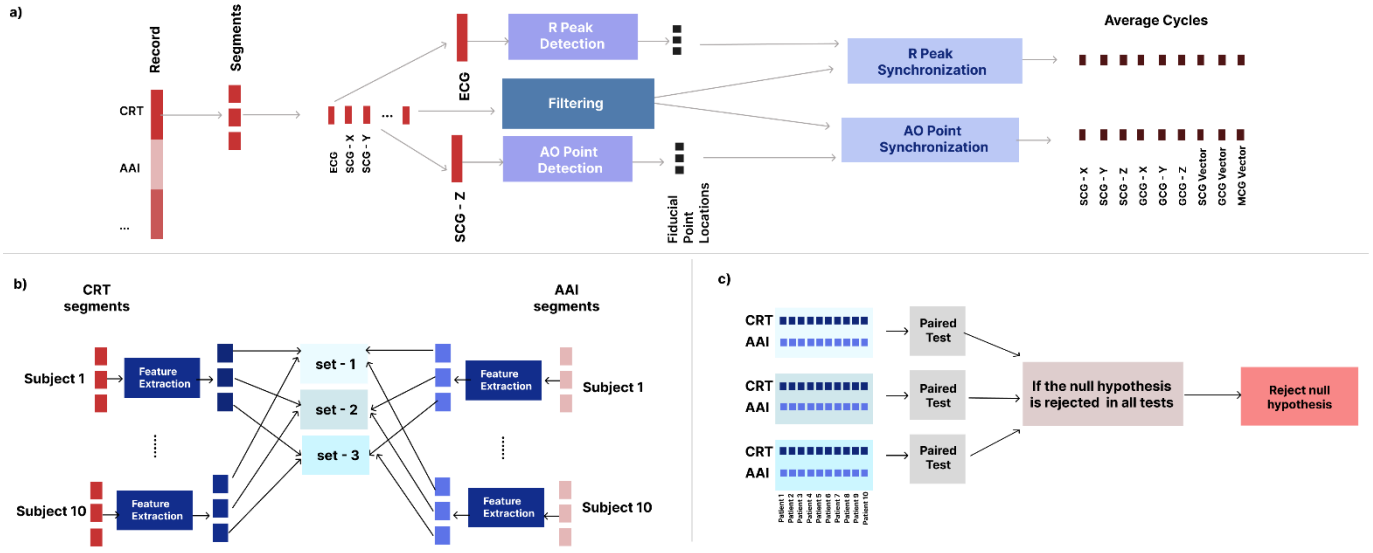

Figure 2 2 (a). The signal processing pipeline. For each patient, three segments were extracted from recordings with AAI and CRT pacing modes and the fiducial points of the segments were detected. For each axis in the segment, we extracted the synchronized averages according to the detected fiducial points and the average cycles were then passed through to the feature extraction pipeline. 2 (b). Distribution of the segments to different sets. For each subject, features of the first, second, and third segments of the corresponding mode are distributed into *set-1*, *set-2*, *set-3* respectively. 2 (c). Data analysis algorithm. A statistical test was performed on each of the separate paired sets, and we rejected the null hypothesis if the null hypothesis is rejected all parallel tests.

All recordings were performed in supine position after 15 minutes rest in a quiet environment. Patients were asked to breath normally and avoid talking and unnecessary movements. Pacemaker was programmed in a random order to AAI or CRT mode and heart rate was set at 80 bpm to get similar stable heart rate during the whole recording. In AAI mode, only atrium is paced leading to dyssynchronic ventricular function and optimized CRT mode should resynchronize the ventricular contraction caused by intraventricular block.

A custom-designed device was used to collect measurements. The device included a 3-axis accelerometer (ADXL355, Analog Devices Inc., Wilmington, MA, USA), a 3-axis gyroscope (LSM6DS3, STMicroelectronics, Geneva, Switzerland), and a single-lead ECG. The device was designed for short data acquisition and not continuous use. Accelerometer and gyroscope measurement ranges were +−2 g and +−250 dps respectively. Noise density of the accelerometer was 25 µg/√Hz and rate noise density of the gyroscope was 7 mdps/√Hz.

The measurements were taken with the sensor placed on the lower portion of the chest with double-sided tape without hair removal (Fig. 1). Each measurement included one accelerometer and one gyroscope signal for each of the 3 axes, and a single-lead ECG. A simultaneous recording of MCG and ECG was conducted.

2.3 Preprocessing & Feature Extraction

Total duration of the recordings in our dataset ranged from 8 minutes to 12 minutes. A resampling to 400 Hz and synchronization operation were performed on the ECG and MCG signals. Segments with motion artifact or low signal quality were excluded manually. Thereafter, a 30-second segment was randomly selected to represent each pacing mode in the final analyses and three successive 10-second segments were extracted from these 30-second segments to enrich our analysis. As a result, for each subject, we extracted six segments; three in the AAI mode and three in the CRT mode.

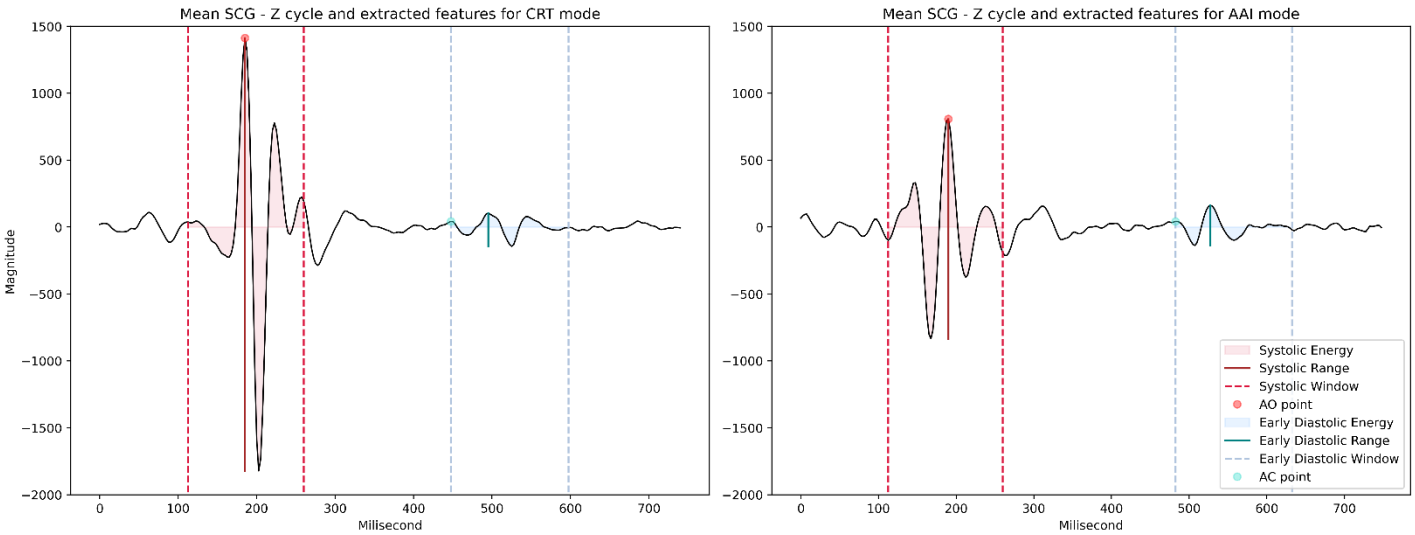

Figure 3 Waveform analysis to show the definitions of extracted features of interest from AO point averaged SCG-Z cycles in a heart failure patient while on CRT pacing (left panel) and AAI pacing mode (right panel).

Each segment contained seven signals; ECG, SCG-X, SCG-Y, SCG-Z, GCG-X, GCG-Y, and GCG-Z.

Four different fiducial points, Q wave, R-peak, aortic valve opening (AO), aortic valve closure (AC), were identified and used in the analysis. For each segment of ECG signal, R-peaks were detected using the algorithm proposed by Hamilton and Q waves were detected using the wavelet based ECG delineation algorithm available in NeuroKit2 toolbox [17–19]. Q wave and R-peak detection in ECG were followed by a peak search in the SCG-Z axis. In the literature, peak detection in SCG-Z axis was used for estimating AO and AC locations and based on that study, each AO was identified as the maximum peak of the SCG-Z signal within the first 125 ms after the corresponding R-peak [16]. The search window for AC point was based on left ventricular ejection time index (LVETI) and LVET reported in the literature [20,21]. Accordingly, the AC was located as the maximum peak of the SCG-Z cycle in interval between 240–300 ms after corresponding AO.

We detected all R-peaks and AO points within each 10-second segment. For extracting a representative cycle for each axis to be used in the feature extraction, each axis of SCG and GCG signals were filtered with a first order Butterworth filter with a passband of one from the following options 20-90 Hz, 6-90 Hz, 1-20 Hz, or >1 Hz (high pass). As an additional step, we created SCG and GCG vector signals by combining all SCG and GCG axes using the Euclidean formula to represent the total movement of the SCG and GCG sensors. MCG vectors were also created by accounting for range differences among the measurement units, scaling SCG and GCG vectors to the [0,1] range using the maximum and minimum values computed for the entire set of vectors within the respective frequency ranges, and subsequently combining them with the Euclidean formula. Subsequently, we extracted average cycles in each axis by aligning the detected R peaks and AO points separately. At the end of this step, we ended up with a dataset that contained 12 average cycles for each individual axis and vector signal, i.e an R-peak and an AO point averaged cycles were calculated for each of the 6 segments of the corresponding signal (6 segments * 2 different average cycles = 12 cycles).

We aimed to reveal differences between CRT and AAI mode comparing their MCG waveforms. Inline with this objective, we needed to define systolic and early diastolic regions on signals by detecting AO and AC points on SCG-Z averages before the feature extraction pipeline. AO points were already known for AO point averaged cycles since they were matched in a specific point during synchronization operation. We detected AO points on R-peak synchronized averages and AC points on

both R-peak and AO point averaged cycles according to our definition. We performed the peak detection operations only on the SCG-Z signals and used same locations on the other axes that was acquired from the same segment and synchronized with the same reference with the corresponding SCG-Z signal. For each of the average cycles, two windows with duration of 150 ms were created. One window was centered on the detected AO as described in the previous study but with a shorter window [22] to avoid the noise of more distant parts and the other window was placed right after AC to focus on early diastolic region (Fig. 3).

The windows around AO and after AC were referred as systolic and early diastolic window, respectively. In feature extraction step, we extracted energy and vertical range of the signals in the systolic and early diastolic windows. Energy (Ex) and vertical range (Rx) were defined as

$$Ex = \sum_{n=-\infty}^{\infty} |x[n]^2| \quad Rx = \max(x[n]) - \min(x[n])$$

Additionally, we extracted left ventricular ejection time (LVET) and electromechanical systole (QS2) by computing the time interval from detected AO to AC and the time interval from Q wave to AC, respectively. The extracted systolic and early diastolic features are shown in the Fig 3. Finally, we added all extracted features in 9 axes (3 SCG axes, 3 GCG axes, 1 SCG vector, 1 GCG vector, and 1 MCG vector) to our feature set for each segment that represented separate parts of the recording and differed based on pacing mode and timing in the recording (Fig. 2 (b)).

2.2 Data Analysis

We aimed to search for potential differences in the MCG waveform between CRT and AAI modes in all SCG and GCG axes, by using varying filtering options and synchronized averaging methods which differ in terms of their reference fiducial point used in the synchronization. For each distinct experiment, we put the corresponding features of the first, second, and third segments of CRT and AAI mode into the set-1, set-2, and set-3, respectively. Hereby, three separate paired sets were constructed, each consisting of one value pair for each subject (Fig. 2 (b)). The paired tests were then applied to evaluate the presence of statistical differences within each set. With this analysis protocol, we aimed to double-check the validity of our results by repeating the experiments on three separate time segments of the recordings.

Statistical comparisons between the pacing modes were performed by using Wilcoxon signed-rank test [23] and $p < 0.05$ as a significance threshold. The differences between pacing modes were considered significant only when the null hypothesis was rejected in all distinct paired tests. If all of the tests did not result in the rejection of the null hypothesis, we did not accept and report the alternative hypothesis (Fig. 2 (c)).

3. Results

The vertical range (Rx) of systolic contraction during CRT mode pacing was higher than in AAI mode. The difference was significant ($p < 0.05$) in every SCG & GCG axis. SCG, GCG, and MCG vectors exhibited also a consistent vertical range differences during systole (Fig. 4). Similarly, the energy (Ex) of the systolic contraction increased when the pacing mode changed from AAI to CRT. This difference was statistically significant in SCG-Y, SCG-Z, GCG-X and GCG-Y axes, and in SCG, GCG and MCG vectors. The differences were most prominent in the 6-90 Hz frequency band, and visible also when the frequency range was extended. The mean differences of systolic energy and vertical range between the pacing modes are shown in each axis, frequency range and by synchronization method in Figure 4.

The pipeline with R-peak or AO point synchronization showed generally comparable results (Fig 4). The vertical range difference in GCG-Z axis was, however, significant only in R-

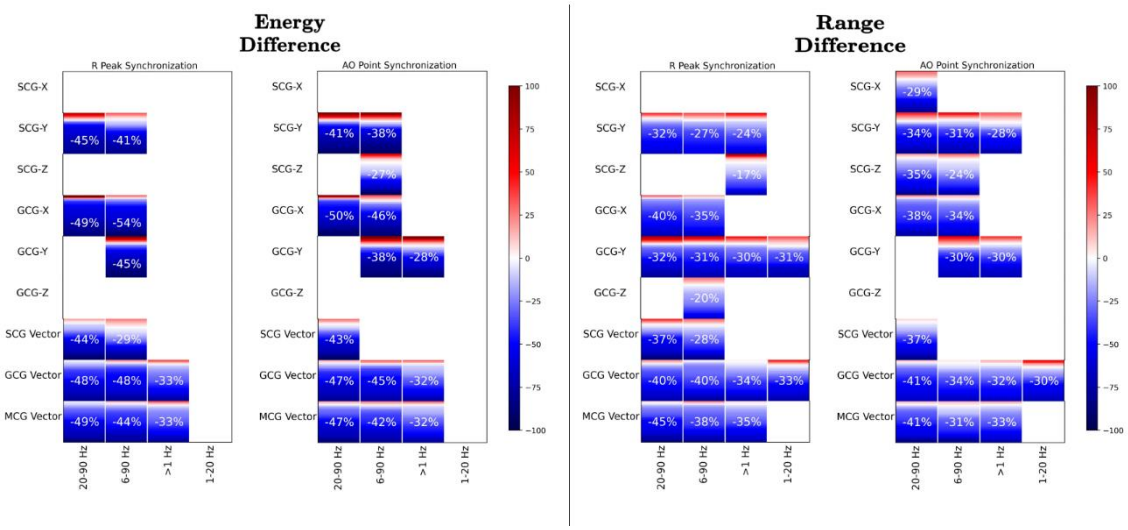

Figure 4 Systolic energy and vertical range differences for each axis, frequency range and synchronization method when the pacemaker mode changed from CRT to AAI. The colored squares show the experiments that showed statistically significant difference between the modes. The percentage in the squares represents the mean change of energy and vertical range after starting AAI pacing, i.e. the difference between CRT and AAI pacing modes relative to the value observed in the CRT mode. Color gradients in each box show the differences between all the CRT-AAI segment pairs of the corresponding experiment settings in descending order.

peak synchronization, while the difference in SCG-X was significant only with AO point synchronization. Mean systolic energy and vertical range differences in GCG-X axis for each subject are presented in Figure 5. In contrast with systolic features, we did not find any consistent differences in energy or vertical range after aortic valve closure between CRT and AAI mode; additionally, the QS2 and LVET were not significantly different between these modes.

4. Discussion

Resynchronization of ventricular function by CRT pacing resulted in concordant changes in MCG signals in all heart failure patients as shown in Figure 5. The consistent finding was a significant increase in systolic energy and range measured from MCG. The differences between the pacing modes were most remarkable in systolic range i.e. maximum peak-to-peak systolic amplitude around AO. SCG-Y, GCG-X & GCG-Y axis together with the frequency range 6-90 Hz were optimal to reveal the differences. On the other hand, we could not observe any consistent changes in any of the early diastolic waveform parameters after resynchronization of ventricular function and no statistically significant difference was detected in the estimated QS2 and LVET.

CRT reduces rate of death and hospitalization in selected patients with HFrEF, improves life quality, and produces reverse remodeling [24–28]. According to the literature, CRT improves the cardiac function by raising the left ventricular ejection fraction, cardiac index, rapid rate of pressure rise (dP/dt) and decreasing left ventricular end-systolic volume index [28–30]. The effect of the CRT was also compared with AAI mode and it was found that CRT resulted with better cardiac function [31]. There is also growing evidence to show that SCG and GCG provide information on left ventricular stroke volume and myocardial contractility [12,22,32–36]. In this study, we analyzed the vertical range (Rx) and energy (Ex) features to represent systolic and early diastolic vibration characteristics in MCG and observed vertical range and energy increases in different axis of MCG signals when pacing mode was changed from AAI to CRT. Based on the earlier research, it is reasonable to conclude that our present observations on changes in systolic waveforms

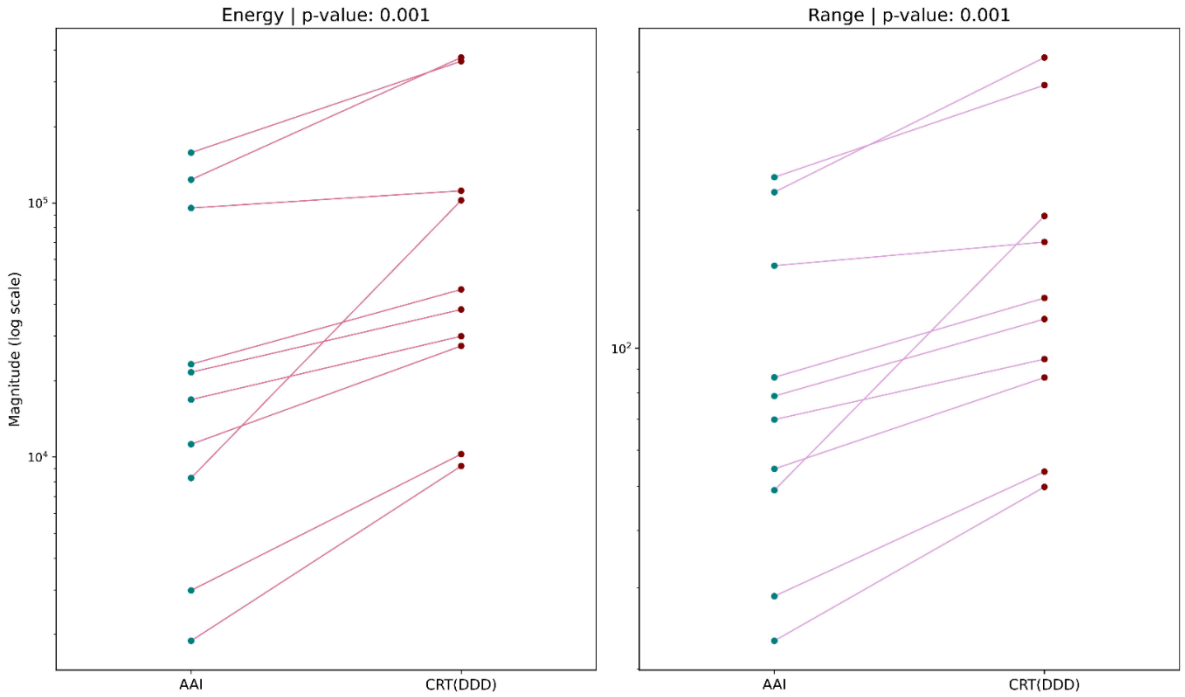

Figure 5 Mean systolic energy and range differences of subjects between 20-90 Hz in GCG-X axis according to AO point synchronization method. The energy and range values shown in the graph were calculated by averaging the whole 30 second segments from the data analysis pipeline.

reflect improvement of ventricular function with CRT pacing and suggest that MCG could be used to assess the efficacy of resynchronization therapy in patients with heart failure.

The first heart sound (S1) has been shown to diminish with reduced cardiac contractility and cardiac reserve and used as a clinical marker of heart failure [37–40]. Consistently, in the present study, the most salient increase in systolic energy during resynchronization was also observed by including the higher SCG and GCG frequencies. Moreover, the changes in systolic components of MCG signals caused by CRT pacing were most prominent in GCG signals which is less sensitive to inter-subject and intra-subject variability than SCG; especially in GCG-X and GCG-Y axis [8,41–44]. The difference was less prominent in GCG-Z axis than other GCG axes since GCG-X and GCG-Y axis are usually of better quality [8]. In addition, among SCG axes, the changes were most remarkable in SCG-Y axis which provides information on foot-to-head direction of blood movements.

Different synchronization reference points can enhance distinct events and information since each axis of MCG sensors shows unique morphology in each hemodynamic event. In the literature, the fiducial points for some MCG axes were already defined [8,45]. Hereby, representative ability of one average cycle for these special morphologies depends on the variability of the distance between the fiducial point and the reference point used for synchronization. The effect of different synchronization references on SCG signal was also shown by Sørensen et al. [45]. For this reason, we used two different synchronization reference points for our analysis. The results when using these synchronizations method were mostly consistent, although differences in SCG-X and GCG-Z axes were statistically significant in only one of the synchronization methods.

On the other hand, we could not observe any consistent changes in any of the early diastolic waveform parameters after resynchronization of ventricular function. Earlier studies have shown that MCG can detect a wide range of abnormalities in

cardiac function caused by myocardial infarction and heart failure [12,15,46–48]. In the literature, a supervised machine learning approach was used and and it is shown that - in line with present findings - the strength features in systolic windows were lower in patients with ST elevation myocardial infarction than in control subjects having normal left ventricular function [49]. The clinical precision of these methods for diagnosis of myocardial infarction or heart failure is, however, limited; inter-individual variation in all signal features is large resulting in significant overlap between the patient groups and healthy controls causing high risk of misclassification for an individual subject. On the other hand, tracking longitudinal changes in SCG and GCG signals in an individual patient may more reliably identify e.g. exacerbation of heart failure or changes of stroke volume [12,16,50]. An audible third heart sound (S3) is a highly specific clinical – but subjective - marker of elevated left ventricular filling pressures in heart failure [51]. In line with this clinical observation, the most significant waveform features reflecting exacerbation of heart failure are observed in early diastole around S3 and seem to be caused by increase in ventricular filling pressures [52–55]. As expected, the early diastolic waveforms did not differ between the pacing modes in the present study, since the compensatory changes in filling pressures to preserve cardiac output take more time to develop.

Earlier studies have shown that LVET in HFrEF patients is significantly shorter than in healthy subjects, and LVET is extended by switching from right ventricular (RV) pacing to CRT [20,21]. However, the difference between mean LVET during CRT and RV-only pacing was only 6 ms and the difference was only significant when measured with impedance cardiography but not with echocardiography [21]. It is essential to note that, in our experiment, all MCG signals were recorded with a 400 Hz sampling frequency, which could potentially pose an obstacle to the sensitive observation of differences in LVET and QS2. In our analysis, no statistically significant difference was observed in the estimated LVET and QS2 in line with previous findings measured on SCG signals recorded with 5000 and 2000 Hz, which indicates that there is no significant difference in LVET between the CRT on - off settings and CRT – AAI pacing [32,56]. Thus, despite that the effects of the CRT mode on systolic performance are salient in MCG, its effects on timing parameters are still ambigious and requires further investigation.

5. Strengths and Limitations

The small number of patients is a limitation and hampers the wider evaluation of potential differences in signal characteristics between CRT responders and non-responders especially in the light of arbitrary definitions of non-responders [57,58]. Secondly, MCG waveform analysis is not automatic. We used a dedicated monitoring device including 1-channel ECG to facilitate identification of fiducial points and the authors were not blinded to the pacemaker setting when annotating the signals. The strength of our experimental design was to provide stable undisturbed conditions including the constant heart rate of 80 bpm and quiet breathing during all MCG recordings. On the other hand, variable increase in sympathetic activity in clinical environment may affect cardiac kinetic energy computed from SCG and GCG and dilute the observed findings [59]. Such effects may lead to differences, even in healthy subjects. Therefore, future studies should concentrate on comparing these differences between healthy subjects and HFrEF patients to assess the significance of our results.

6. Conclusion

Our findings show that the mechanical signals recorded on the lower chest wall with the accelerometers and gyroscopes change significantly during CRT pacing reflecting improvement of mechanical cardiac function with resynchronization therapy. Micro electro mechanical systems (MEMS) together wearable technology enable the introduction of MCG in clinical environment. The

present findings are promising, but larger studies are needed to see whether MCG analysis could help to optimize CRT already during pacemaker implantation and later during follow-up.

7. Acknowledgements

7.1 Disclosures

KEJA: Research grants from the Finnish Foundation for Cardiovascular Research, Lecture fees from Bayer, Pfizer and Boehringer Ingelheim. Member in the advisory boards for Bayer, Pfizer and Astra Zeneca. OL: part-time work at Precordior Ltd. TK: a shareholder of Precordior Ltd.

7.2 Sources of Funding

This study was funded by The Finnish Foundation for Cardiovascular Research, Helsinki, Finland, Clinical Research Fund (EVO) of Turku University Hospital, Turku, Finland, and Business Finland (1788/31/2019)

7.3 Data availability

Access to data is regulated by Finnish law. Data are available from the Turku University Hospital for researchers who meet the criteria as required by the Finnish law to access confidential data. Contact person who will distribute data upon request to qualified researchers: Tuija Vasankari, Msc, Heart Center, Turku University Hospital, PO BOX 52, FIN-20521, Turku, Finland; tuija.vasankari@tyks.fi.

8. References

[1] Authors/Task Force Members, McMurray JJ, et al. ESC Guidelines for the diagnosis and treatment of acute and chronic heart failure 2012: The Task Force for the Diagnosis and Treatment of Acute and Chronic Heart Failure 2012 of the European Society of Cardiology. Developed in collaboration with the Heart Failure Association (HFA) of the ESC. European heart journal. 2012;33(14):1787–847.

[2] Cleland JG, Abraham WT, et al. An individual patient meta-analysis of five randomized trials assessing the effects of cardiac resynchronization therapy on morbidity and mortality in patients with symptomatic heart failure. European heart journal. 2013;34(46):3547–56.

[3] Friedman DJ, Al-Khatib SM, et al. Cardiac Resynchronization Therapy Improves Outcomes in Patients With Intraventricular Conduction Delay But Not Right Bundle Branch Block: A Patient-Level Meta-Analysis of Randomized Controlled Trials. Circulation. 2023;147(10):812–23.

[4] Heggermont W, Auricchio A, et al. Biomarkers to predict the response to cardiac resynchronization therapy. EP Europace. 2019;21(11):1609–20.

[5] Pujol-López M, San Antonio R, et al. Electrocardiographic optimization techniques in resynchronization therapy. EP Europace. 2019;21(9):1286–96.

[6] Hawkins NM, Petrie MC, et al. Selecting patients for cardiac resynchronization therapy: the fallacy of echocardiographic dyssynchrony. Journal of the American College of Cardiology. 2009;53(21):1944–59.

[7] Gurev V, Tavakolian K, et al. Mechanisms underlying isovolumic contraction and ejection peaks in seismocardiogram morphology. Journal of medical and biological engineering. 2012;32(2):103.

[8] Jafari Tadi M, Lehtonen E, et al. Gyrocardiography: A new non-invasive monitoring method for the assessment of cardiac mechanics and the estimation of hemodynamic variables. Scientific reports. 2017;7(1):1–11.

[9] Sieciński S, Kostka PS, et al. Gyrocardiography: A review of the definition, history, waveform description, and applications. Sensors. 2020;20(22):6675.

[10] Jaakkola J, Jaakkola S, et al. Mobile phone detection of atrial fibrillation with mechanocardiography: the MODE-AF Study (Mobile Phone Detection of Atrial Fibrillation). Circulation. 2018;137(14):1524–7.

[11] Morra S, Hossein A, et al. Assessment of left ventricular twist by 3D ballistocardiography and seismocardiography compared with 2D STI echocardiography in a context of enhanced inotropism in healthy subjects. Scientific reports. 2021;11(1):683.

[12] Morra S, Pitisci L, et al. Quantification of Cardiac Kinetic Energy and Its Changes During Transmural Myocardial Infarction Assessed by Multi-Dimensional Seismocardiography. Frontiers in Cardiovascular Medicine. 2021;8:603319.

[13] Halvorsen PS, Fleischer L, et al. Detection of myocardial ischaemia by epicardial accelerometers in the pig. British journal of anaesthesia. 2009;102(1):29–37.

[14] Becker M, Roehl A, et al. Simplified detection of myocardial ischemia by seismocardiography. Herz. 2014;39(5):586.

[15] Inan OT, Baran Pouyan M, et al. Novel wearable seismocardiography and machine learning algorithms can assess clinical status of heart failure patients. Circulation: Heart Failure. 2018;11(1):e004313.

[16] Koivisto T, Lahdenoja O, et al. Mechanocardiography-Based Measurement System Indicating Changes in Heart Failure Patients during Hospital Admission and Discharge. Sensors. 2022;22(24):9781.

[17] Hamilton P. Open source ECG analysis. In IEEE; 2002. p. 101–4.

[18] Makowski D, Pham T, et al. NeuroKit2: A Python toolbox for neurophysiological signal processing. Behavior research methods. 2021;1–8.

[19] Martínez JP, Almeida R, et al. A wavelet-based ECG delineator: evaluation on standard databases. IEEE Transactions on biomedical engineering. 2004;51(4):570–81.

[20] Weissler AM, Harris WS, et al. Systolic time intervals in heart failure in man. Circulation. 1968;37(2):149–59.
[21] Noda K, Endo H, et al. Comparison of the measured pre-ejection periods and left ventricular ejection times between echocardiography and impedance cardiography for optimizing cardiac resynchronization therapy. Journal of arrhythmia. 2017;33(2):130–3.
[22] Jensen AS, Schmidt SE, et al. Effects of cardiac resynchronization therapy on the first heart sound energy. In IEEE; 2014. p. 29–32.
[23] Wilcoxon F. Individual comparisons by ranking methods. Springer; 1992.
[24] Tang ASL, Wells GA, et al. Cardiac-Resynchronization Therapy for Mild-to-Moderate Heart Failure. N Engl J Med. 2010 Dec 16;363(25):2385–95.
[25] Moss AJ, Hall WJ, et al. Cardiac-resynchronization therapy for the prevention of heart-failure events. New England Journal of Medicine. 2009;361(14):1329–38.
[26] Cleland JGF, Daubert JC, et al. The Effect of Cardiac Resynchronization on Morbidity and Mortality in Heart Failure. N Engl J Med. 2005 Apr 14;352(15):1539–49.
[27] Bristow MR, Saxon LA, et al. Cardiac-Resynchronization Therapy with or without an Implantable Defibrillator in Advanced Chronic Heart Failure. N Engl J Med. 2004 May 20;350(21):2140–50.
[28] Linde C, Gold MR, et al. Long-term impact of cardiac resynchronization therapy in mild heart failure: 5-year results from the REsynchronization reVErses Remodeling in Systolic left vEntricular dysfunction (REVERSE) study. European Heart Journal. 2013 Sep 1;34(33):2592–9.
[29] Steendijk P, Tulner SA, et al. Hemodynamic effects of long-term cardiac resynchronization therapy: analysis by pressure-volume loops. Circulation. 2006;113(10):1295–304.
[30] Yu CM, Chau E, et al. Tissue Doppler echocardiographic evidence of reverse remodeling and improved synchronicity by simultaneously delaying regional contraction after biventricular pacing therapy in heart failure. Circulation. 2002;105(4):438–45.
[31] Leclercq C, Cazeau S, et al. Acute hemodynamic effects of biventricular DDD pacing in patients with end-stage heart failure. Journal of the American College of Cardiology. 1998;32(7):1825–31.
[32] Sørensen K, Søgaard P, et al. Seismocardiography as a tool for assessment of bi-ventricular pacing. Physiological Measurement. 2022;43(10):105007.
[33] P. Castiglioni, A. Faini, et al. Wearable Seismocardiography. In: 2007 29th Annual International Conference of the IEEE Engineering in Medicine and Biology Society. 2007. p. 3954–7.
[34] K. Tavakolian, A. P. Blaber, et al. Estimation of hemodynamic parameters from seismocardiogram. In: 2010 Computing in Cardiology. 2010. p. 1055–8.
[35] Gemignani V, Bianchini E, et al. Transthoracic sensor for noninvasive assessment of left ventricular contractility: validation in a minipig model of chronic heart failure. Pacing and clinical electrophysiology. 2010;33(7):795–803.
[36] Bordachar P, Labrousse L, et al. Validation of a new noninvasive device for the monitoring of peak endocardial acceleration in pigs: implications for optimization of pacing site and configuration. Journal of cardiovascular electrophysiology. 2008;19(7):725–9.
[37] Thakur PH, An Q, et al. Haemodynamic monitoring of cardiac status using heart sounds from an implanted cardiac device. ESC heart failure. 2017;4(4):605–13.
[38] Hansen PB, Luisada AA, et al. Phonocardiography as a Monitor of Cardiac Performance During Anesthesia. Anesthesia & Analgesia [Internet]. 1989;68(3). Available from: https://journals.lww.com/anesthesia-analgesia/Fulltext/1989/03000/Phonocardiography_as_a_Monitor_of_Cardiac.37.aspx
[39] Xiao S, Guo X, et al. A relative value method for measuring and evaluating cardiac reserve. BioMedical Engineering OnLine. 2002 Dec 6;1(1):6.
[40] Zheng Y, Guo X, et al. Computer-assisted diagnosis for chronic heart failure by the analysis of their cardiac reserve and heart sound characteristics. Computer methods and programs in biomedicine. 2015;122(3):372–83.
[41] Tadi MJ, Lehtonen E, et al. Gyrocardiography: A new non-invasive approach in the study of mechanical motions of the heart. Concept, method and initial observations. In IEEE; 2016. p. 2034–7.
[42] Tadi MJ, Lehtonen E, et al. A miniaturized MEMS motion processing system for nuclear medicine imaging applications. In IEEE; 2016. p. 133–6.
[43] O. Lahdenoja, T. Humanen, et al. Heart rate variability estimation with joint accelerometer and gyroscope sensing. In: 2016 Computing in Cardiology Conference (CinC). 2016. p. 717–20.
[44] O. Lahdenoja, T. Hurnanen, et al. Atrial Fibrillation Detection via Accelerometer and Gyroscope of a Smartphone. IEEE Journal of Biomedical and Health Informatics. 2018 Jan;22(1):108–18.
[45] Sørensen K, Schmidt SE, et al. Definition of fiducial points in the normal seismocardiogram. Scientific reports. 2018;8(1):15455.
[46] Blomster J, Lahdenoja O, et al. CardioSignal Smartphone Application Detects Atrial Fibrillation in Heart Failure Population. Circulation. 2021;144(Suppl_1):A12517–A12517.
[47] S. Mehrang, O. Lahdenoja, et al. Classification of Atrial Fibrillation and Acute Decompensated Heart Failure Using Smartphone Mechanocardiography: A Multilabel Learning Approach. IEEE Sensors Journal. 2020 Jul 15;20(14):7957–68.
[48] Hossein A, Mirica DC, et al. Accurate Detection of Dobutamine-induced Haemodynamic Changes by Kino-Cardiography: A Randomised Double-Blind Placebo-Controlled Validation Study. Scientific Reports. 2019 Jul 19;9(1):10479.
[49] Koivisto T, Lahdenoja O, et al. Mechanocardiography in the Detection of Acute ST Elevation Myocardial Infarction: The MECHANO-STEMI Study. Sensors. 2022;22(12):4384.
[50] Shandhi MMH, Fan J, et al. Estimation of changes in intracardiac hemodynamics using wearable seismocardiography and machine learning in patients with heart failure: a feasibility study. IEEE Transactions on Biomedical Engineering. 2022;69(8):2443–55.
[51] Marcus GM, Gerber IL, et al. Association between phonocardiographic third and fourth heart sounds and objective measures of left ventricular function. Jama. 2005;293(18):2238–44.
[52] Capucci A, Santini L, et al. Preliminary experience with the multisensor HeartLogic algorithm for heart failure monitoring: a

retrospective case series report. ESC heart failure. 2019;6(2):308–18.
[53] Sandler R, Gamage P, et al. Potential SCG Predictors of Heart Failure Readmission. Journal of Cardiac Failure. 2020 Oct 1;26(10, Supplement):S87.
[54] Joshi N. The third heart sound. Southern medical journal. 1999;92(8):756–61.
[55] Mehta NJ, Khan IA. Third heart sound: genesis and clinical importance. International journal of cardiology. 2004;97(2):183–6.
[56] Marcus Fi, Sorrell V, et al. Accelerometer-Derived Time Intervals during Various Pacing Modes in Patients with Biventricular Pacemakers: Comparison with Normals. Pacing and Clinical Electrophysiology. 2007 Dec 1;30(12):1476–81.
[57] Tomassoni G. How to define cardiac resynchronization therapy response. J Innov Card Rhythm Manag. 2016;7:S1-7.
[58] Boidol J, Średniawa B, et al. Many response criteria are poor predictors of outcomes after cardiac resynchronization therapy: validation using data from the randomized trial. EP Europace. 2013 Jun 1;15(6):835–44.
[59] Morra S, Gauthey A, et al. Influence of sympathetic activation on myocardial contractility measured with ballistocardiography and seismocardiography during sustained end-expiratory apnea. American Journal of Physiology-Regulatory, Integrative and Comparative Physiology. 2020;319(4):R497–506.